Numerical Study of Non-Premixed Combustion Characteristics on Supplementary Firing of HRSG

Teguh Hady Ariwibowo*(1), Arrad Ghani Safitra(2), Muhammad Haidar Fakri (3), Muhammad Aghist Fitrony(4)
[1,2,4] *Department of Energy Mechanical Engineering, Politeknik Elektronika Negeri Surabaya*, Surabaya, Indonesia
[3] *PT. PAL Indonesia*, Surabaya, Indonesia
Email address: ***teguhhady@pens.ac.id**

***Abstract*— Computational fluid dynamics (CFD) is a simulation model to provide complex processes in the industry that has been widely used to investigate industrial-scale combustion phenomena. Supplementary firing is used to increase steam production. The non-premixed combustion is a type of supplementary firing. Supplementary firing has seven burners arranged vertically. Supplementary firing uses exhaust steam from a gas turbine to ignite the air. This research investigates the combustion characteristics of flame length and exhaust gas emission at burners. The viscous model was observed by using non-premixed modeling. While the absorption of radiation in the combustion residual gas was observed by using the weight sum-gray gases model (WSGGM). This study used the realizable *k-ε* model and tetrahedron meshing algorithm to approach the turbulent characteristics. The total nodes and the orthogonal mesh quality in the meshing steps are 1,334,359 and 0.86, respectively. The modeling results show that burners-1 and 7 have longer flame compared to other burners. The combustion exhaust gas has height contents of CO_2 and H_2O. The velocity near the furnace wall is lower than the center of the furnace, but the pressure is higher. This phenomenon is dominantly influenced by the thermal boundary layer.**

Keywords— Supplementary firing, flame length, exhaust gases, combustion

I. INTRODUCTION

Combustion is one of the research objects in computational fluid dynamics (CFD) modeling. In general, combustion is the result of rapid chemical reactions which is currently a hot topic for observation. Exhaust emissions, flame length and heat transfer are the results of the combustion process. Internal combustion, especially non-premixed, has been extensively studied by researchers related to the supplementary firing type in heat recovery steam generator (HRSG). Supplementary firing has function to increase steam production. Supplementary firing utilizes exhaust gas from gas turbine (GT) for air combustion.

Granados and co-wokers [4] used CFD analysis to investigate the combustion phenomenon in a rotary cement, namely recirculation. The remaining combustion gases were used for the combustion process and the combustion air had been mixed with the exhaust gases. The study aimed to determine the combustion temperature, radiation and convection heat transfer, and the flame length. It revealed that the highest temperature results occurred at a concentration of 85%. Similarly, the convection and radiation heat transfer are also reduced. According to this study, the most optimal concentration was at 85%.

In another study, Nemitallah and Habib [5] used CFD analysis to investigate the combustion phenomenon in the gas turbine combustion chamber. The study varied the equivalent ratio and then assessed the concentration of combustion air O_2 and CO_2 in volume percentage. They observed the effect of these variations on the temperature, velocity, mole fraction, and emission distribution in the exhaust gas combustion chamber. The concentration ratio of O_2/CO_2: 60%/40% had the highest axial velocity compared to other variations. Air discharge also increased the axial velocity. The highest O_2 concentration caused the exhaust gas values (H_2O, CO_2, CO) to show the highest graph trend. This phenomenon was related to the ideal combustion.

Based on the previous research, this study aims to observe the combustion phenomenon in the HRSG owned by PT KDM (Kaltim Daya Mandiri), Bontang, East Kalimantan. There are seven burners built into the HRSG. Supplementary firing uses exhaust gas from GT for the combustion process. This study will observe the combustion characteristics, flame length phenomena and emission gas combustion.

II. METHODS

The research method is divided into two parts, namely numerical simulation settings and furnace geometry
Numerical modeling iss carried out using the Reynolds-Averaged Navier-Stokes equation for the continuity equation (1) and the momentum equation (2). Double precision pressure-based is used as a solver. The second order upwind and PRESTO! are used to determine pressure. This model is chosen because it is very suitable for flowing fluids. The fluid is assumed to be incompressible flow. The SIMPLE algorithm is used for the pressure-velocity coupling equation [6] - [8].

$$\frac{\partial}{\partial x_i}(\rho u_i) = 0 \tag{1}$$

$$\frac{\partial}{\partial x_j}(\rho u_i u_j) = -\frac{\partial \rho}{\partial x_i} + \frac{\partial}{\partial x_j}\left[\mu\frac{\partial x_i}{\partial x_j} + \frac{\partial x_j}{\partial x_i} - \frac{2}{3}\delta_{ij}\frac{\partial u_l}{\partial x_l}\right] + \frac{\partial}{\partial x_j}\left(-\rho\overline{u_i' u_j'}\right) \tag{2}$$

https://jurnal.polines.ac.id/index.php/eksergi

ISSN 0216-8685 (print); 2528-6889 (online)

M. Ghadamgahi et al have reported comparisons of standard and realizable *k-ε* in oxy-fuel combustion [9]. It was found that the realizable *k-ε* value was better for non-premixed combustion. This has also been reported by several reports in the use of realizable *k-ε* [6], [9]. The realizable *k-ε* equation is as follows:

$$\frac{\partial(\rho\varepsilon)}{\partial t}+\frac{\partial(\rho\varepsilon u_j)}{\partial x_j}=\frac{\partial y}{\partial x_j}\left[\left(\mu+\frac{\mu_t}{\sigma_\varepsilon}\right)\frac{\partial\varepsilon}{\partial x_j}\right]+\rho C_1 S_\varepsilon-\rho C_2\frac{\varepsilon^2}{k+\sqrt{\nu\varepsilon}}+C_{1\varepsilon}\frac{\varepsilon}{k}C_{3\varepsilon}G_b \quad (3)$$

$$C_1=max\left[0.43,\frac{\eta}{\eta+5}\right] \quad (4)$$

$$\eta=S_\varepsilon^k \quad (5)$$

$$S=\sqrt{2S_{ij}S_{ij}} \quad (6)$$

where $\sigma_k=1;\ \sigma_3=1{,}2;\ C_2=1{,}9;\ C_{1\varepsilon}=1{,}44, and\ C_{3\varepsilon}$ is:

$$C_{3s}=tanh\left|\frac{v_i}{u_\perp}\right| \quad (7)$$

The radiation model in this study used Radiative Transfer Equation model. This model is used to specify the opaque walls in the interior domain. The transfer equation is used for a finite number of discrete solid angles. The following equation is used for the contribution of phase particles:

$$\nabla\overrightarrow{Is}+(a+a_p+\sigma_s)I(\vec{r}.\vec{s})=an^2\frac{\sigma T^4}{\pi}+E_p+\frac{\sigma_p}{4\pi}+\int_0^{4\pi}I(\vec{r}.\vec{s})\phi(\vec{s}.\vec{s})d\Omega' \quad (8)$$

where the values of α, αp are the absorption coefficient of gas and particle, σs and σp are the scattering coefficients of gas and particles. Ep is the equivalent of particle emission. σ is the Boltzmann constant, I is the radiation intensity, T is the local temperature, Φ is the phase scaling function, Ω is the solid angle. DO (Discrete Ordinates) is used in oxy fuel combustion [4] [10], [11],[14].

The high-efficient of non-premixed combustion is caused by the involvement of several transport equation solutions for one or two scalar equations from the equation species. Scalar conservation is a mixed fraction which is defined as a fluid thermochemical reaction [15]. The mixed fraction can be expressed by the atomic mass fraction [4], as shown in the equation (9),

$$f=\frac{Z_i-Z_{i,0x}}{Z_{i,fuel}-Z_{i,ox}} \quad (9)$$

Equation (9) shows the oxidation value at the inlet stream and the equation for the fuel value at the inlet stream. If the diffusion value is assumed in the same value, then the equation can be simplified into a single equation for the mixture fraction (*f*). This equation is also suitable for turbulent flow [4], [12]. This modeling is a thermochemical scalar (species fraction, density and temperature) which is combined into a mixture fraction in the probability density function (PDF). This modeling is used as a sub-grid consideration of local fluctuations between species and is further explained by beta-functions and the PDF experimental process. The following is the equation for the Favre mean (density-averaged) mixture fraction:

$$\frac{\partial}{\partial}(\rho\bar{f})+\nabla.(\rho\bar{v}\bar{f})=\nabla\left[\frac{\mu_t}{\sigma_t}\nabla\bar{f}\right]+S_m+S_{user} \quad (10)$$

S_m is the mass transfer from the reaction of liquid phase or other phases to the gas phase. In simple terms, the equation is described as follows:

$$\frac{\partial}{\partial}(\rho\overline{f'^2})+\nabla.(\rho\bar{v}\overline{f'^2})=\nabla\left[\frac{\mu_t}{\sigma_t}\nabla\overline{f'^2}\right]+C_g\mu_t(\nabla\bar{f})^2-C_d\rho\frac{\varepsilon}{k}\overline{f'^2}+S_{user} \quad (11)$$

The weight sum-gray gases model is used to predict the heat flux on the walls and radiation sources [9], [13]. The sequence for the absorption of combustion gases is very important to see the dispersion in the furnace in the equation (12):

$$\varepsilon=\sum_{i=0}^{I}a_{\varepsilon,i}(T)(1-e^{-k,p\vec{s}} \quad (12)$$

$a_{\varepsilon,i}$ is the emissivity of the weighted factor for gray gas and the quantity k_i is the absorption coefficient for gray gas. *p* is the partial pressure for all absorbed gases, and $\vec{S}$ is the path length [9].

One of the pre-processing stages is the geometry drawing. This study uses a 3-dimensional model with a scale of 1:1. Geometry is made by simplifying several parts. Figure 1 shows the geometry of the furnace with the seven burners. Air Inlet 1 is exhaust gas from GT which enters the furnace, and it is located behind the burner. Air inlet 2 is also an exhaust gas from GT which has an inlet angle near the nozzle. The burner nozzle has a size of 10 mm. The geometry of the furnace is 14 m long and 4.17 m wide.

The boundary conditions are determined based on the existing input. Figure 1 shows the boundary conditions used in this study. The boundary conditions in this study are based on the input parameters of the industrial datasheet of PT. KDM at a load of GT 100. There are five boundary conditions that must be defined. Pressure air inlets 1 and 2 enter the furnace at 2451 Pa and temperature at 685 K. The nozzle has an outlet pressure of 1.5 bar and a temperature of 300 K. The walls of the furnace are made of steel with a temperature of 1000 K. The outlet has a pressure of 2000 Pa. The hydraulic diameter is used as a turbulence model because it is an internal flow.

The air and fuel compositions are listed in Table 1. The fluid mixture is a mixture of combustion air and fuel using PDF. The WSGGM model is used to absorb radiation in a fluid mixture. Several studies have used this model because of its good accuracy.[6], [8]

Meshing used is a tetrahedron with the number of nodes 1,334,359. The results of the orthogonal quality show the

https://jurnal.polines.ac.id/index.php/eksergi

ISSN 0216-8685 (print); 2528-6889 (online)

number 0.86 which indicates the quality of the meshing is very good. The node value is calculated based on the Rajhi approach.

Rajhi and co-workers evaluated several types of radiation models to find out the best approximation model through experiments. They use a 3-dimensional model with a scale of 1 and the number of nodes is 1,335,180 [7].

Table 1
Boundary conditions

	Nozzle Burner	Air Inlet 1	Air Inlet 2	Furnace Wall	Outlet
Boundary conditions	Inlet pressure	Inlet pressure	Inlet pressure	Wall	Outlet pressure
Total pressure (Pa)	150,000	2451	2451	-	2000
Temperature (K)	300	685	685	1000	1000
Turbulence models	Intensity and hydraulic diameter	Intensity and hydraulic diameter	Intensity and hydraulic diameter	-	Intensity and hydraulic diameter
Hydraulic diameter (m)	0.01	1.67	0.185	-	6.49
Material	mixture	mixture	mixture	steel	mixture
Concentrations	CO_2:4,984% CH_4:86,039 % C_2H_6:3,974% C_3H_8:2,808% iC_4H_{10}:0,596 % nC_4H_{10}:0,710 % iC_5H_{12}:0,285 % nC_5H_{12}:0,186 % C_6^+:0.353%	O_2:13,45 % N_2:72,56 % Ar:0,87% CO_2:3,24 % H_2O:9,56 %	O_2:13,45 % N_2:72,56 % Ar:0,87 % CO_2:3,24% H_2O:9,56%		

.

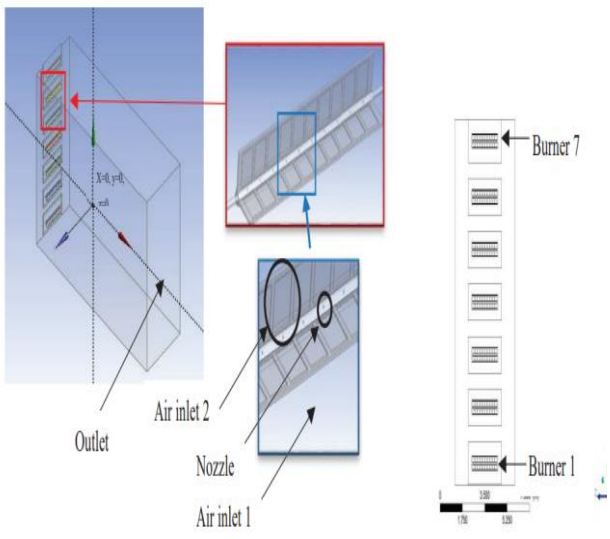

Fig. 1. Boundary conditions, combustion chamber and burner geometry

III. Results and Discussions

The CFD model was validated using the of pressure and temperature data from PT KDM datasheet. The pressure at points x=-3.76, y=-3.83, z=-1.26 (Figures 2 and 3) on the model show the pressure of 1894.39 Pascal. At the same point, the datasheet shows a pressure of 2000 Pa which results in a deviation of 5.28%. The temperature at the point x=-3.76, y=4.60, z= -1.26 (Figures 2 and 3) which shows a temperature of 1156.31 K. While the measured temperature is 1123 K. The temperature deviation shows an error of 2.90%.

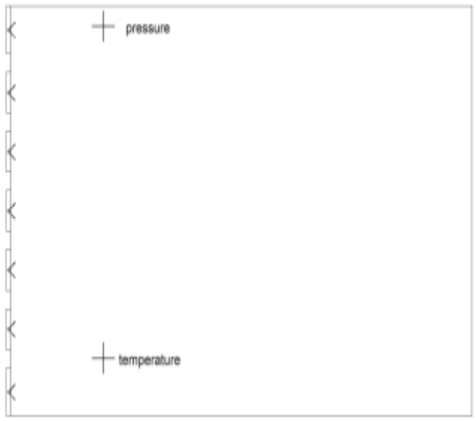

Fig. 2. Sample position for temperature and pressure validation in the xy-plane

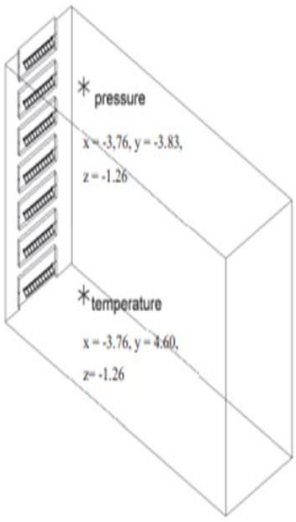

Fig. 3. Validation based on 3D visualization

Figure 4 shows the flame temperature on the seven burners, where burner 1 and burner 7 have a higher temperature than the other burners. Burner 7 has the highest temperature of 1570 K and it is located in the front of burner. The average temperature of all burners is 1420 K. On x-direction, the temperature continues to decrease. This is also experienced in every burner.

Figures 9 and 10 show the flame length. The burner 1 has flame length of 4.5 m and burner 7 has flame length of 4.4 m. Table 2 shows the comparison of the longest flame to other burners. The flame length is influenced by the value of oxygen concentration [4]. In Figure 5a the oxygen value in burners 1 and 7 is less than in other burners. Burner 1 and burner 7 are located below and above the furnace walls. The

https://jurnal.polines.ac.id/index.php/eksergi

ISSN 0216-8685 (print); 2528-6889 (online)

flame length is also influenced by the thermal boundary layer which results in inhibiting the velocity of the fluid flow. Figures 6 and 7 show the vectors and contours of the velocity. The velocity near the wall has low value. Thermal boundary layer inhibits the fluid velocity. Figure 8 shows the lower high pressure on the furnace wall due to the higher velocity and lower pressure in the center of furnace. Burner 1 and burner 7 take longer time to reach the fully developed phase.

Tabel 2
Flame length, highest temperature and average temperature

Burner No.	Flame length (m)	Highest temperature (K)
Burner 1	4.50	1809.18
Burner 2	2.30	1802.93
Burner 3	2.38	1791.65
Burner 4	2.55	1651.92
Burner 5	2.51	1801.98
Burner 6	2.35	1790.66
Burner 7	4.4	1804.07
Average	3.3	1778.93

Exhaust emissions from the combustion are shown in Figures 5b and 5c. It indicates the presence of CO_2 and H_2O. The emission score is determined based on the results of combustion. In this case, burner 7 has 0.17 mol% CO_2 and 0.07 mol% H_2O which is the highest compared to other burners. These results are followed by burner 1 which has high emissions as well. Burners 1 and 7 were found to be better than other burners, seen from the high concentration of O_2 at the lowest position of the potential core. These results explain that the emission value plays an important role in producing complete combustion.

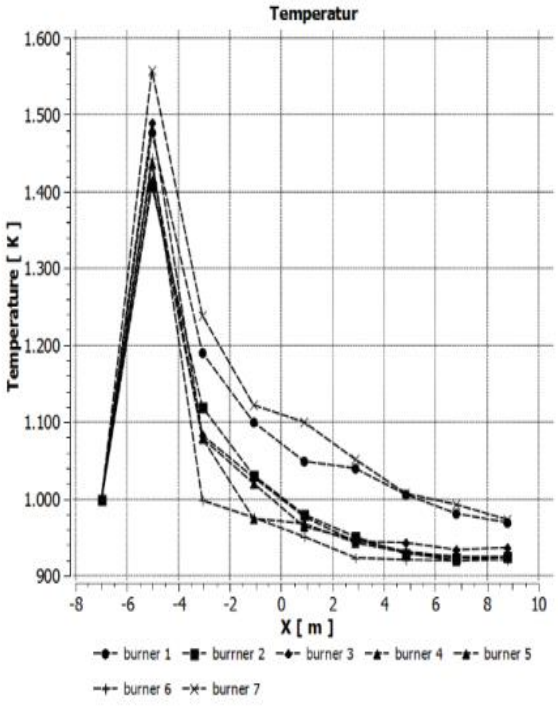

Fig. 4. Distribution of combustion temperature

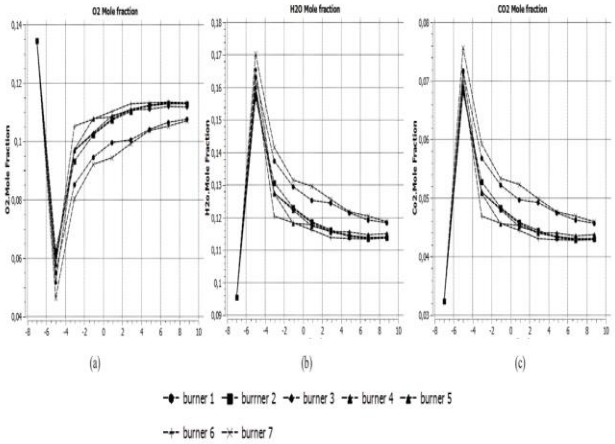

Fig. 5. Combustion gas distribution of (a) O_2 mol % (b) H_2O mol% (c) CO_2 mol %

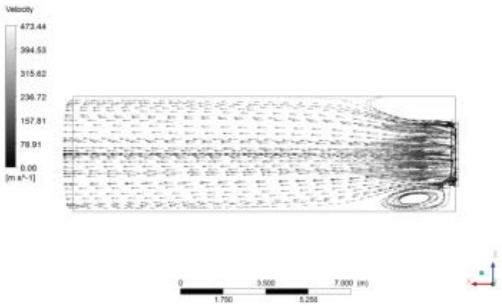

Fig. 6. Velocity vector on the top burner

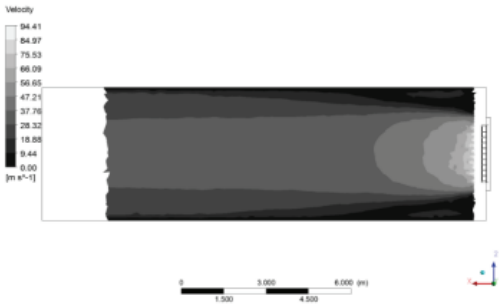

Fig. 7. Vector velocity of zx-plane at y = 4.5

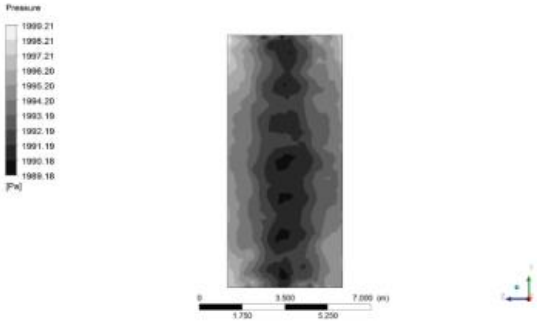

Fig. 8. Pressure contour of yz-plane at x = 0

https://jurnal.polines.ac.id/index.php/eksergi

ISSN 0216-8685 (print); 2528-6889 (online)

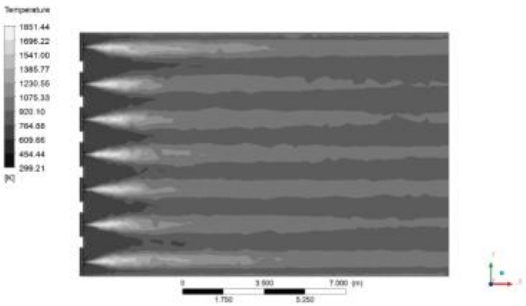

Fig.9. Pressure contour of xy-plane at z = -1.13

IV. CONCLUSIONS

This study aims to observe the combustion phenomenon in the furnace. By using the data obtained from the company's datasheet, the phenomenon of temperature and flame length in each burner has been investigated. The highest temperature and flame length were observed at the bottom (4.4 m) and above (4.5 m) burner. Similar evidence was also found that the combustion emissions of CO_2 (0.07 mol%) and H_2O (0.17 mol%) were higher than other burners. The flame rate and pressure near the walls tend to be slower and higher than at the center of furnace. This phenomenon occurs due to the influence of the thermal boundary layer.

REFERENCES

[1] E. Eduardo & S. Lora (2003) , "INFLUENCE OF AMBIENT TEMPERATURE IN COMBINED CYCLE," vol. i, no. 1999.

[2] P. Ahmadi & I. Dincer (2011), "Thermodynamic analysis and thermoeconomic optimization of a dual pressure combined cycle power plant with a supplementary firing unit," ENERGY Convers. Manag., vol. 52, no. 5, pp. 2296–2308.

[3] V. Ganapathy (2014), Steam Generators and Waste Heat Boilers: For Process and Plant Engineers.

[4] D. A. Granados, F. Chejne, J. M. Mejía, C. A. Gómez, A. Berrío, and W. J. Jurado (2014), "Effect of flue gas recirculation during oxy-fuel combustion in a rotary cement kiln," Energy, vol. 64, pp. 615–625.

[5] M. A. Nemitallah & M. A. Habib (2013), "Experimental and numerical investigations of an atmospheric diffusion oxy-combustion flame in a gas turbine model combustor," Appl. Energy, vol. 111, pp. 401–415.

[6] R. Prieler, B. Mayr, M. Demuth, D. Spoljaric, & C. Hochenauer, (2015). "Application of the steady flamelet model on a lab-scale and an industrial furnace for different oxygen concentrations," Energy, vol. 91, pp. 451–464.

[7] M. A. Rajhi, R. Ben-Mansour, M. A. Habib, M. A. Nemitallah, & K. Andersson. (2014). "Evaluation of gas radiation models in CFD modeling of oxy-combustion," Energy Convers. Manag., vol. 81, pp. 83–97.

[8] R. Prieler, B. Mayr, M. Demuth, B. Holleis, & C. Hochenauer. (2016). "Prediction of the heating characteristic of billets in a walking hearth type reheating furnace using CFD," Int. J. Heat Mass Transf., vol. 92, pp. 675–688.

[9] M. Ghadamgahi, P. Ölund, T. Ekman, N. Andersson, & P. Jönsson. , (2016). "A Comparative CFD Study on Simulating Flameless Oxy-Fuel Combustion in a Pilot-Scale Furnace," J. Combust., vol. 2016, pp. 1– 11.

[10] E. Karampinis, N. Nikolopoulos, A. Nikolopoulos, P. Grammelis, & E. Kakaras. (2012). "Numerical investigation Greek lignite/cardoon co-firing in a tangentially fired furnace," Appl. Energy, vol. 97, pp. 514–524.

[11] H. B. Vuthaluru & R. Vuthaluru. (2010). "Control of ash related problems in a large scale tangentially fired boiler using CFD modelling," Appl. Energy, vol. 87, no. 4, pp. 1418–1426.

[12] S. Septiawan. (2013). "Numerical Study of Characteristic Natural Gas Combustion in Furnace Boiler with Various Swirl Angle Vanes at Radially Stratified Flame Core Burners," vol. 2, no. 1.

[13] R. Johansson, K. Andersson, B. Leckner, & H. Thunman. (2010). "Models for gaseous radiative heat transfer applied to oxy-fuel conditions in boilers," Int. J. Heat Mass Transf., vol. 53, no. 1–3, pp. 220–230.

[14] X. Yang, Z. He, Q. Niu, S. Dong, & Heping Tan. (2019). "Numerical analysis of turbulence radiation interaction effect on radiative heat transfer in a swirling oxyfuel furnace," Int. J. Heat Mass Transf., vol. 141, pp. 1227–1337.

[15] S. Echi, A. Bouabidi, Z. Driss, & M. S. Abid.(2019) "CFD simulation and optimization of industrial boiler," Energy, Vol 169, pp 105-114

https://jurnal.polines.ac.id/index.php/eksergi

ISSN 0216-8685 (print); 2528-6889 (online)